Interaction between Undersaturated Polymer Layers: Computer Simulations and Numerical Mean-Field Calculations

Jorge Jimenez,[†] Jason de Joannis,[†] Ioannis Bitsanis,[‡] and Raj Rajagopalan*[,†]

Department of Chemical Engineering, University of Florida, Gainesville, Florida 32611-6005, and Foundation for Research and Technology, Hellas Institute of Electronic Structure & Laser, P.O. Box 1527, Heraklion 711 10, Crete, Greece

Received June 27, 2000; Revised Manuscript Received September 5, 2000

ABSTRACT: Lattice Monte Carlo simulations and the contact distribution method are used to analyze the force of interactions between two undersaturated polymer layers in good solvents. The net force between the surfaces, resulting from a competition between bridging attraction and steric repulsion, is obtained unambiguously for coverages Γ ranging from 0 to the saturation coverage Γ_0. The sizes and the number of the bridges are in qualitative agreement with previous scaling analysis, but a number of quantitative differences important in practice emerge from the simulations. While the bridges may be considered as independent elastic tethers at low coverages, steric interactions begin to exert influence for coverages as low as $\Gamma \approx 0.3\Gamma_0$. Comparison of the results of the simulations with numerical mean-field calculations based on second-order Markov chains (i.e., without backfolding) shows good agreement with some of the structural features of the polymer layer, but important discrepancies regarding the force of interaction exist for all values of Γ/Γ_0. Whereas the mean-field calculations predict that the crossover from attraction to steric repulsion occurs only near saturation, the simulations show the crossover to occur at a much higher degree of undersaturation (i.e., $\Gamma/\Gamma_0 \approx 0.85$). The simulation method used provides an opportunity to scrutinize systematically the details of the mean-field theory and to refine the theory for providing better guidance in practice. The results presented here focus on a low molecular weight chain ($N = 200$). Whether the asymptotic behavior for very long chains predicted by the scaling/free energy functional approach is obtained still needs to be tested.

1. Introduction

The interactions between polymer-bearing surfaces play a central role in a large number of chemical, biological, and materials sciences and processes. Detailed knowledge of the structure of polymer layers and polymer-induced forces is therefore essential for tailoring polymer additives in an increasing number of scientific and technological applications (e.g., colloid stabilization, lubrication, etc.).

Two main groups of theories, commonly referred to as "scaling" and "mean-field" theories, have been used to provide guidelines on the layer structure and induced forces and to interpret experimental measurements. In general terms, mean-field theories for polymer adsorption extend the standard Flory−Huggins picture of polymer solutions to allow for the calculation of free energies in systems with concentration gradients (e.g., at solid/liquid or liquid/liquid interfaces). Early work in this area is based on the Cahn−de Gennes approach, which uses a free energy functional that contains both an interaction energy term and a configurational energy term (i.e., the square gradient term).[1,2] This approach, which leads to the so-called ground state dominance approximation, has been used to analyze polymer layers under good,[2] Θ,[3] and poor solvent[4,5] conditions. More recently, Semenov and Joanny[6,7] used a self-consistent approach based on the Edwards propagation equation and two order parameters to describe the concentration profile near an interface, as opposed to just one parameter as used in the ground state dominance approximation. Their approach, which is strictly valid for the marginal solvent regime,[8] allows for the determination of tail-dominant and loop-dominant regions and the determination of asymptotic laws for the density of loops, tails, and free chains.

The use of a mean-field theory to describe a polymer layer relies on the assumption that spatial fluctuations in the local segment density are negligible. This assumption breaks down under good solvent conditions, when the structure of the layer resembles that of a semidilute polymer solution. The scaling approach developed by de Gennes[9] is intended to address that particular situation. By considering that the structure of a layer under such conditions is self-similar (i.e., the spatial correlation length, ξ, is directly proportional to the distance from the surface, z), de Gennes obtained simple scaling laws for the density profile and the force of compression.[9,10] In an attempt to obtain more precise formulas, de Gennes proposed a "scaling-based" free energy functional as a substitute for the mean-field free energy functional used in the Cahn−de Gennes approach. This so-called *renormalized* mean-field theory (also called "scaling" theory) was able to reproduce the predictions from scaling arguments.[1] This approach has since been extended by Rossi and Pincus[11−13] to the case of unsaturated polymer layers.

One drawback of the above-mentioned studies is that they are valid only for infinitely long chains. In this context, an important complement to the analytical mean-field theories is the numerical lattice mean-field theory of Scheutjens and Fleer (SF theory).[14] In the original formulation, the SF theory considers a first-order Markov chain in a self-consistent mean-field potential. (A first-order Markov chain admits backfolding of segments, although such backfolding is physically forbidden.) Comparison with the analytical theories has

[†] University of Florida.
[‡] Institute of Electronic Structure & Laser.

10.1021/ma0011237 CCC: $19.00 © 2000 American Chemical Society
Published on Web 10/13/2000

shown that the (mean-field) asymptotic laws for long polymers are obtained only when the chains contain several thousand statistical segments,[15,16] which correspond to a molecular weight that is well beyond the molar mass of the polymer additives that are commonly used in practice.

Several extensions have been developed for the standard SF theory.[17] Some of these extensions consider the chain statistics in terms of a second-order Markov process (i.e., a chain which avoids backfolding)[18,19] and also the use of a self-consistent anisotropic (mean-field) model (a model that takes into account bond correlations and attempts to improve over the random mixing approximation).[19−21] A careful analysis of the conditions for which the numerical predictions are valid and, additionally, an understanding of the deviations of these predictions (in those situations where mean field is not appropriate) are of utmost importance. In this context, computer simulations become an ideal tool to generate unambiguous results, which can then be used to undertake the above-mentioned scrutiny.

A first step in this direction was taken by de Joannis and Bitsanis,[22] who performed a careful examination of the structure of a polymer layer in equilibrium with a bulk solution for a wide range of adsorption energies and molecular weights. These authors used lattice Monte Carlo simulations and a technique based on the "configurational bias" algorithm of Siepmann and Frenkel,[23] which allows for an efficient sampling of the conformations of confined or physisorbed polymer chains. We have recently combined this technique with the contact distribution method[24,25]—an efficient method to estimate differences in the Helmholtz potential from lattice Monte Carlo simulations—to examine the structure and forces induced by a single chain confined between athermal walls,[26] a single chain confined between two adsorbing walls,[27] and a polymer layer confined by a bare surface.[28]

In this paper we extend our previous work to examine the interactions between two physisorbed layers with surface coverages Γ ranging from 0 to the saturation coverage Γ_0 (defined near the end of the next section). One of our objectives is to complement the study of bridging due to *isolated* polymer chains we had initiated earlier.[27] In addition, we wish to examine the competition between bridging attraction and steric repulsion that occurs between undersaturated polymer layers. We also provide a detailed comparison between the simulation results and the numerical mean-field predictions based on first-order (standard SF theory) and second-order Markov chains (hereinafter referred to as SF_1 and SF_2, respectively). As noted above, the former tolerates the backfolding of chain segments, while the latter eliminates such backfolding.

2. Model and Simulation Method

The computational method used here consists of three steps: (i) generation of polymer configurations using Monte Carlo simulations, (ii) determination of force of interaction (i.e., change in the Helmholtz potential as the two polymer-bearing surfaces approach each other), and (iii) calculation of the same quantities using self-consistent mean-field theory. In all cases, the space is discretized using a simple cubic lattice, and the polymer chains are modeled as appropriate lattice random walks. Some additional details follow below.

2.1. Lattice Model. We model the polymer chains as self-avoiding walks (SAW's) inscribed on a simple cubic lattice with dimensions $L \times L \times H$. Periodic boundary conditions are used in the x and y directions, whereas two impenetrable walls confine the layers in the z direction. The two walls are adsorptive, with the discrete surface/segment potential given as

$$U_{\text{ext}} = \begin{cases} \infty & z < 1,\ z > H \\ -\epsilon & z = 1,\ z = H \\ 0 & 1 < z < H \end{cases} \quad (1)$$

The number of steps N is chosen as 200 in each SAW.[29] A general background on lattice Monte Carlo models of polymers can be found in ref 30.

For the numerical mean-field calculations shown in section 3.3, we keep the same underlying lattice structure (i.e., simple cubic) and the same adsorption energy ϵ and chain length N used in the simulations. In this case, however, the polymers are considered as first- or second-order Markov chains (in contrast to simulations, where the chains are essentially $(N-1)^{\text{st}}$-order Markov chains), and the excluded-volume interactions are taken into account using a mean-field assumption. Additional details on the numerical mean-field calculations have been presented by Scheutjens and co-workers.[14,18]

2.2. Simulation Method for Structure and Forces. For generating equilibrium conformations of the polymer chains, we have employed the configurational bias method.[23] In this method, sampling of the SAW's consists of breaking an existing chain configuration into two parts, erasing one of these subchains, and randomly regrowing it using an algorithm based on the well-known Rosenbluth−Rosenbluth method.[31]

For exact calculation of forces of interaction from the Monte Carlo simulations, we have used a new, versatile method, known as the contact distribution method (CDM), introduced recently by Jimenez and Rajagopalan.[24,25] The calculation of forces from simulations of continuous (off-lattice) models makes use of a well-established method based on the calculation of the pressure from the virial theorem.[32] In a lattice model, however, the force, f, needs to be estimated from the derivative of the Helmholtz potential, F, with respect to a relevant coordinate. For instance, in our case, the force exerted by the polymer chains when the separation between the walls is decreased from H to $H-1$ is given as

$$f(H - {}^1/_2) = -\frac{\partial F}{\partial h}\Big|_{H-1/2} \approx F(H-1) - F(H) \quad (2)$$

defined such that a negative force implies an attraction between the walls. Here, h is used to represent the wall separation as a free variable.[33] As noted above, the calculation of the Helmholtz energy difference in eq 2 is obtained using CDM, the contact distribution method. To obtain the Helmholtz energy difference, the CDM requires the determination of the distribution of the number of contacts between the polymer chains and the surface. This distribution of contacts represents the probability, $p(m)$, of finding m segments in the surface layer (i.e., at $z = H$). We have recently demonstrated the use of this method and its value by considering a number of problems of practical interest, e.g., (i) the force of compression of end-grafted chains by finite-sized objects,[24,34] (ii) the force of confinement of a single chain between two "athermal" walls,[26] and (iii) the bridging attraction induced by a single chain confined between two adsorptive walls.[27]

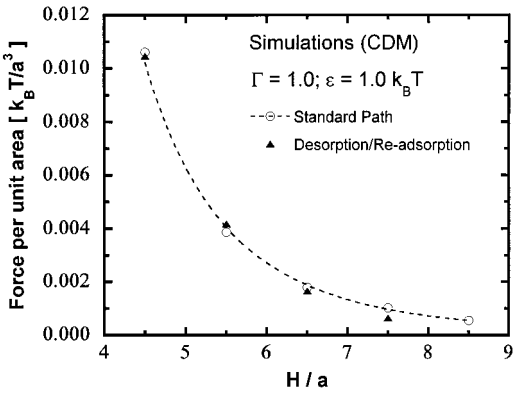

Figure 1. Compression of a polymer layer by an "athermal" (neutral) wall, illustrating two different ways of determining the force of confinement. The surface coverage on the adsorptive surface (with adsorption energy $\epsilon = 1.0\ k_BT$) is $\Gamma = 1.0$ monolayer.

In the present case, to examine the interaction between two surfaces bearing physisorbed polymers, we need to follow a somewhat circuitous path between the initial state (where the layers are separated by H lattice units) and the final state (where the layers are separated by $H - 1$ lattice units). As the Helmholtz potential is a state function, the actual path used to calculate the energy difference in eq 2 is immaterial and can, in fact, be "unphysical". This path consists of three steps: (i) desorption of the chains from one of the walls (taken to be the upper one here), (ii) moving that wall to the new position, and (iii) readsorption of the chains back on that wall. To achieve this, the calculation requires the use of a sequence of fictitious potentials at the upper surface, $U_{ext}(z=H)$. During step i, $U_{ext}(H)$ is gradually increased, starting from $-\epsilon$, until the probability of zero surface contacts is obtained accurately. Once this probability is determined with sufficient accuracy, the energy change corresponding to the compression is obtained as described by Jimenez and Rajagopalan.[24,25] The energy change determined in this manner characterizes the difference in Helmholtz potential that occurs when the adsorptive wall moves by one lattice unit and simultaneously becomes nonadsorptive. Step ii therefore corresponds to a polymer system of width $H - 1$, in equilibrium with one adsorptive wall (the lower one) and one nonadsorptive wall (the upper one). Finally, in step iii the surface potential at the upper wall, $U_{ext}(H - 1)$, is gradually decreased[35] from 0 to $-\epsilon$, so that the chains are readsorbed at the upper wall. The sum of the free energy changes obtained in these steps is the desired total change in the Helmholtz energy.

Although, from a fundamental point of view, the desorption/readsorption approach is valid, the propagation of errors in such a calculation may raise questions concerning the accuracy of this methodology. Therefore, to test the accuracy of the proposed method, we have calculated the force of compression between a polymer layer and an athermal (neutral) wall following two different paths. In the first and more direct path, we "move" the bare surface. In this case, we only need to determine the probability of zero surface contacts,[36] $p(0)$. In the second and more tortuous path, we move the surface with the adsorbed chains (i.e., we first "desorb" the chains, and then we "move" the wall and then readsorb the chains, referred to as the desorption/readsorption path). The results of such a calculation are shown in Figure 1. It is clear from the figure that the agreement between the two approaches is very good and that the methodology used to estimate forces between two physisorbed layers is indeed valid. The size of the lattice (L) used for all the simulations presented in this paper is $L/a = 40$, where a is the lattice spacing. The number of polymer chains was varied from $n = 1$ to $n = 20$ in order to obtain different coverages on the surfaces. We define the surface coverage Γ as the total number of segments belonging to adsorbed chains divided by the area of the adsorptive surfaces (i.e., it represents the number of monolayers adsorbed on each surface). For instance, the results presented in Figure 1 correspond to a surface coverage $\Gamma = 1.0$ monolayer. The number of polymer chains used in that particular simulation[37] was $n = 8$.

It is also useful to think in terms of the surface coverage Γ relative to the equilibrium coverage Γ^* that one would obtain when the surface is in contact with a polymer solution. Since Γ^* is a function of the bulk concentration ϕ_b of the solution, it is common practice to define a *saturation* coverage Γ_0 as the coverage obtained when $\phi_b \rightarrow 0$. This definition presents no problem when the chain length N approaches infinity, since the adsorption isotherm (i.e., a plot of Γ^* as a function of ϕ_b) looks essentially like a step function. For "short" chains, however, one obtains Γ_0 from the extrapolation of Γ^* (beyond the initial rise) to $\phi_b = 0$. For instance, for the system under study (i.e., $N = 200$ and $\epsilon = 1.0\ k_BT$), the saturation coverage corresponds to 1.2 monolayers, as determined by de Joannis and Bitsanis.[22]

3. Interaction between Two Undersaturated Surfaces

In the first part of this section we focus on the number of bridges and the average size of bridges as functions of the surface coverage Γ and the separation between walls H/a. The chain length of the polymers used in this study is $N = 200$, and the adsorption energy is $\epsilon = 1.0\ k_BT$. This section is intended to complement our previous work on bridging by a single polymer chain. In particular, we want to determine the surface coverage at which the steric repulsion sets in. Following this, we examine the competition between steric repulsion and bridging attraction between two undersaturated surfaces and compare our results with numerical self-consistent calculations using first-order Markov chains (standard SF theory, denoted henceforth as SF_1) and second-order Markov chains (SF_2), the latter to eliminate chain backfolding.

3.1. Structure of Bridges. 3.1.1. Bridging Due to Single Chains. When the surface coverage is very small, bridging between two surfaces may occur due to isolated polymer chains. This limiting case has been examined by Ji et al.,[38] who presented analytical results based on scaling arguments for the average size (i.e., average number of segments contained in the bridge) l_{br} and the average number of bridges n_{br}, i.e.,

$$n_{br} \sim N\left(\frac{D}{a}\right)^{-5/3} \exp(-H/2D) \tag{3}$$

and

$$l_{br} \sim \left(\frac{D}{a}\right)^{5/3}\frac{H}{D} \tag{4}$$

where N is the chain length, a is the monomer size, and D is a length comparable to the average loop extension,

which depends only on the adsorption energy. To estimate the forces due to bridging, Ji et al. assumed each bridge to be individually governed by the Pincus law of elasticity.[39] In our context, the Pincus law is

$$f = C\frac{(H-1)^{3/2}}{R_{\mathrm{br}}{}^{5/2}} \tag{5}$$

where, for our lattice model, $H - 1$ is the stretched end-to-end distance of the bridge, R_{br} is the unperturbed end-to-end distance of a chain containing as many segments as there are in each bridge, and C is a proportionality constant.[40] This assumption yields a force per bridge that is independent of the separation distance H between the surfaces,

$$f_{\mathrm{br}} \sim D \tag{6}$$

or

$$f_{\mathrm{br}} \sim \left(\frac{\epsilon}{a}\right)^{3/2} \tag{7}$$

since $D \sim (\epsilon/a)^{3/2}$, as shown by de Gennes.[9]

The case of a semidilute solution confined between two adsorbing walls has also been considered by Ji et al.,[38] who, to make predictions for the force due to bridging, have assumed that each bridge is still governed by the Pincus law. The discussion they present in this context is, however, speculative. In this case, one would expect the steric interactions to play a major role, and hence, it is unlikely that the system will behave as a collection of elastic tethers.

3.1.2. Bridging in Undersaturated Layers. In our earlier work, we examined the case of bridging by a single polymer chain. We presented computer simulation results for the number and size distribution of bridge conformations and the resulting attractive force between the surfaces as a function of intersurface distance H/a and adsorption energy ϵ. These results showed that in the case of strong adsorption ($\epsilon > 0.5\ k_{\mathrm{B}}T$) the force per bridge f_{br} is indeed independent of separation and depends only on the adsorption energy, in good agreement with the scaling predictions. In this section we extend our previous work to examine the structure of the bridges and the forces induced by undersaturated polymer *layers*. The adsorption energy used in all our simulations is $\epsilon = 1.0\ k_{\mathrm{B}}T$.

In Figure 2 we plot the average number of bridges n_{br} as a function of H/a for different values of the surface coverage Γ (given in number of monolayers). The broken line in this figure represents the single-chain results obtained from our earlier work, which was done with a polymer chain consisting of 1000 segments (and the same adsorption energy, $\epsilon = 1.0\ k_{\mathrm{B}}T$). As evident from the figure, for low values of Γ (up to $\Gamma = 0.5$), the average number of bridges shows the same exponential decay with H. As the coverage is increased beyond $\Gamma = 0.5$, we observe a slower (almost) exponential decay (i.e., with a larger decay length). As pointed out by Ji et al., the blob size (which determines the rate of exponential decay in eq 3) cannot be determined unambiguously in systems with two similar characteristic lengths. When the chains remain isolated, the only characteristic length in the system is the layer thickness D (which depends only on the adsorption energy). As the surface coverage is increased, spatial fluctuations in the system

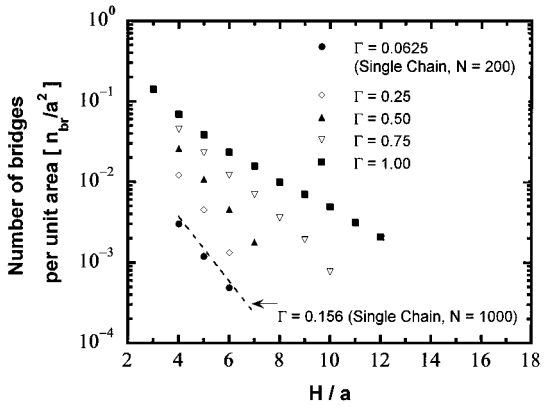

Figure 2. Number of bridges n_{br} per unit area as a function of the separation between surfaces H/a (where a is the lattice spacing).

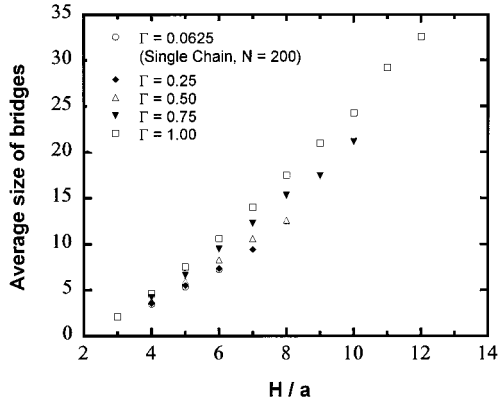

Figure 3. Average size of bridges l_{br} (i.e., average number of segments within a bridge) as a function of the separation between surfaces, H/a (where a is the lattice spacing).

(which are characterized by the mesh size ξ) become important and cause a deviation from eq 3. Ji et al.[38] speculate that when $\xi < D$, the decay length is given by ξ (instead of D), which would decrease with increase in surface coverage. Figure 2 appears to contradict the suggestion of Ji et al., but no definitive conclusions can be drawn without data for larger Γ's.

A similar situation can be observed from Figure 3, which shows the average size of the bridges as a function of H/a. The results show a linear relation between l_{br} and H/a. For low coverages, this relation is characterized only by the layer thickness D. Similar to Figure 2, the deviations in the slope are evident for $\Gamma > 0.5$.

A more interesting situation arises when one compares the bridging force directly obtained from the simulations with that estimated from the number and size distribution of bridges (i.e., following the assumption that each bridge is individually governed by the Pincus law). This comparison is presented in Figure 4, which shows the force per bridge f_{br} obtained at a fixed intersurface distance ($H/a = 4.5$) as a function of the surface coverage Γ. The force per bridge is defined as the ratio of the total force to the number of bridges obtained from the simulation. The solid line in the figure corresponds to the estimation based on the number and size distribution of the bridges.[27,43] The deviation between the two curves indicates the onset of the steric repulsion between the layers. (A similar behavior is observed in our work on bridging by a single chain for low adsorption energies, i.e., $\epsilon \leq 0.5\ k_{\mathrm{B}}T$.) The fact that

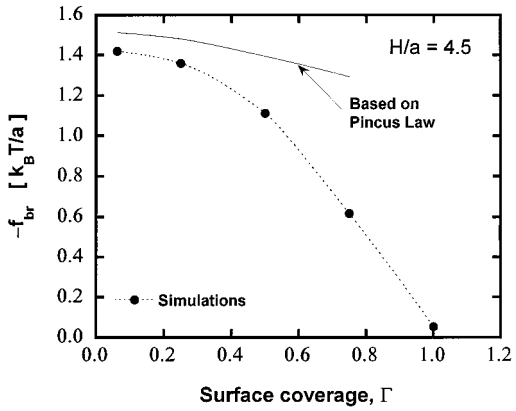

Figure 4. Force per bridge f_{br} versus Γ for a fixed separation distance between the surfaces ($H/a = 4.5$).

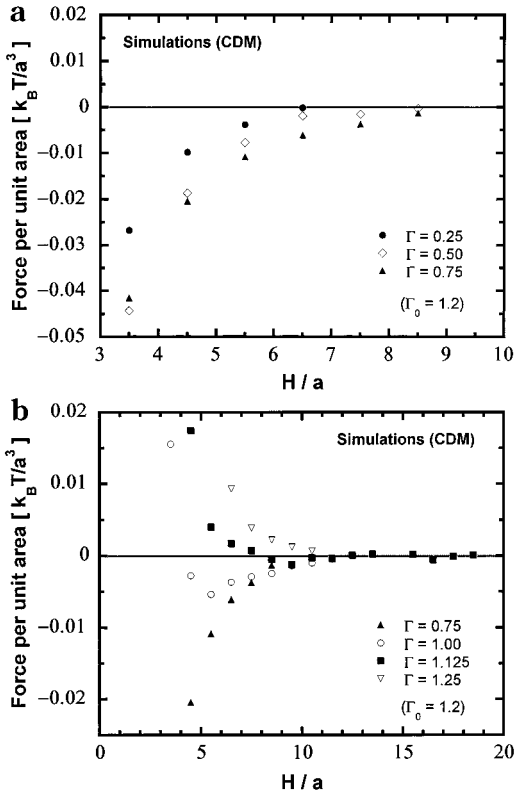

Figure 5. Force per unit area f versus H/a for a range of surface coverage Γ between 0 and Γ_0: (a) Γ between 0 and 0.75; (b) Γ between 0.75 and 1.25.

f_{br} obtained directly from simulations is approximately constant as $\Gamma \rightarrow 0$ indicates that for very low coverages the surface can be considered as a collection of isolated polymer chains. In this regime f_{br} is determined by the segment−surface adsorption energy. As the coverage is increased, steric repulsion sets in, and the ratio between the total force and the number of bridges loses its meaning.

3.2. Competition between Bridging Attraction and Steric Repulsion. The force profiles obtained for different surface coverages are shown in Figure 5a,b. As discussed in the previous section, at very low coverages the surface can be seen as a collection of isolated polymer chains. An increase in the coverage gives rise to an increase in the attractive force, as seen in Figure 5a, because of the increase in the number of bridges (see, for example, Figure 2). As the surface coverage increases further, the polymer chains begin to overlap, and a competition between bridging attraction and steric repulsion sets in. In addition, the average size of the bridges also increases, and the attractive force therefore extends to a longer range (see Figure 5a).

For further increases in Γ, the steric repulsion becomes dominant, and a decrease in the attractive force is observed (see Figure 5b). For a particular coverage ($\Gamma \sim 1.12$ in our case), the net force between the walls becomes roughly zero (except at very close distances where a steep repulsion is always observed). It is interesting to note that the value of Γ for which the force essentially vanishes is below the saturation coverage Γ_0. (As mentioned earlier, Γ_0 was obtained from the extrapolation of the adsorption isotherm to $\phi_b = 0$. For $N = 200$, $\epsilon = 1.0\ k_BT$; $\Gamma_0 = 1.2$ monolayers.) Any increase in the coverage beyond the saturation value results in a steric repulsion at all distances.

At this point it is interesting to comment on the predictions based on the "scaling"/free energy functional for undersaturated layers. As pointed by Rossi and Pincus,[11,12] a coverage lower than Γ_0 results, essentially, in a decrease in the repulsion between the surfaces. Only when the relative surface saturation Γ/Γ_0 becomes lower than 0.4 does the net force become attractive (in contrast to simulations where forces become attractive for relative saturations at $\Gamma/\Gamma_0 \approx 0.85$). We note, however, that the chain length used in this study is not large enough to test the asymptotic predictions of the scaling theory; therefore, the discrepancy mentioned earlier deserves further attention.

3.3. Comparison with Numerical Mean-Field Theory. It is instructive and important to compare the results of our simulations with the predictions of the numerical mean-field theory of Scheutjens and Fleer,[14] as the latter are the only predictions available for "short" polymers. Such a comparison can be used to identify the most useful refinements needed for improving the accuracy of the numerical lattice mean-field theory. The original formulation of Scheutjens and Fleer is based on the conformations of a first-order Markov chain subject to a mean-field potential. As well-known,[44] this formulation contains two critical assumptions, namely, (i) random mixing of segments in each layer and (ii) the possibility of chain backfolding. In this paper, in addition to examining the original formulation, we also relax the second assumption by using a second-order Markov chain for the step-weighted walk representing the polymer chains. This extension of the standard SF theory was introduced by Scheutjens and Leermakers[18] and later used by van der Linden et al.[19] to examine the adsorption of semiflexible copolymers.

As an illustration, we first present, in Figure 6a,b, the number and size of the bridges as functions of H/a for a surface coverage of $\Gamma = 0.75$. These figures show the results obtained from simulations and the ones calculated for a first-order (SF_1) and a second-order (SF_2) Markov chain. The improvement introduced by the second-order Markov chain is evident (especially at close separations), both in the number and in the size of the bridges. More interesting, however, is the comparison of the prediction for the force, shown in Figure 7. The differences in this case are drastic, with the simulations giving rise to a much stronger attractive force than the ones predicted by SF_1 or SF_2. The force shown in Figure 7 is the result of bridging and steric contributions. Although the numerical mean-field calculations based on the second-order Markov chain (SF_2) yields good

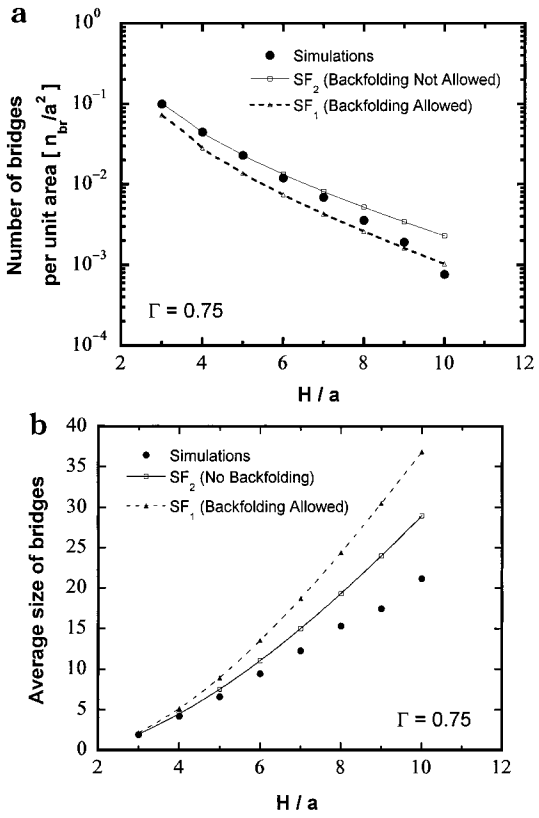

Figure 6. Structural properties of the bridges: (a) average number of bridges n_{br} per unit area as a function of H/a for $\Gamma = 0.75$; (b) average size of bridges l_{br} as a function of H/a for $\Gamma = 0.75$.

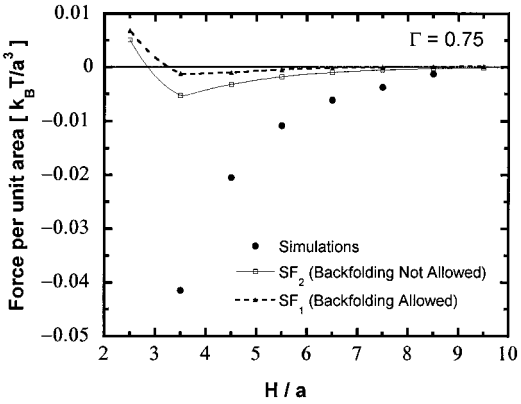

Figure 7. Force per unit area between walls f versus separation, H/a, for $\Gamma = 0.75$.

predictions of the structural properties of bridges, the underestimation of the saturation coverage Γ_0 affects the steric contribution to the force.

To better illustrate the differences in the predictions, we show in Figure 8a the net force at a close separation ($H/a = 4.5$) as a function of Γ. First, this figure illustrates several of our previous observations. At low coverages (where the surface consists of isolated polymer chains) one observes a linear increase in the (attractive) force with a corresponding increase in coverage. In this regime, the forces are mainly due to intrachain interactions. The comparison between the predictions of SF_1 and SF_2 also confirms our previous observations that the use of a second-order Markov chain improves the standard SF theory (i.e., SF_1) substantially. In particular, the linearity of the attractive force with coverage is captured by SF_2, although

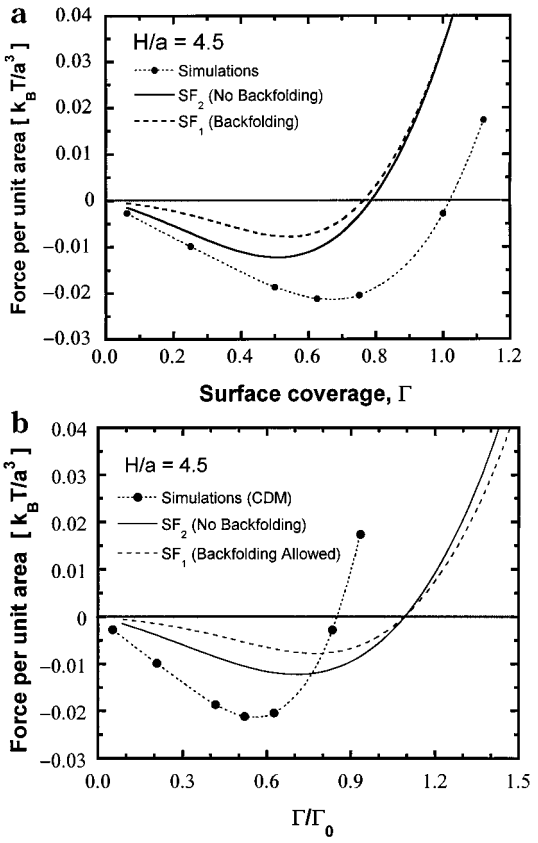

Figure 8. (a) Force per unit area at fixed separation ($H/a = 4.5$) as a function of surface coverage, Γ. (b) Force per unit area at fixed separation ($H/a = 4.5$) as a function of the relative surface coverage, Γ/Γ_0.

SF_2 still falls short of the expected magnitude and the rate of increase, as predicted by the simulations. As the coverage is increased further, one observes a much larger deviation between mean-field calculations and computer simulations. The forces predicted by SF_1 and SF_2 become repulsive at lower coverages as compared to simulations, which is something one would expect due to the fact that the mean-field theories *underestimate* the saturation coverage. For instance, for $N = 200$ and $\epsilon = 1.0\ k_BT$, the saturation coverage obtained from mean-field calculations is $\Gamma_{0,SF_1} = 0.7$ for the first-order Markov chain and $\Gamma_{0,SF_2} = 0.72$ for the second-order Markov chain, in contrast to $\Gamma_{0,sim} = 1.2$ obtained from simulations.

Because of the differences in the saturation coverages obtained from the mean-field theory and the simulations, one would expect a better agreement if the forces are compared for the same *relative* surface saturation Γ/Γ_0. To examine this, we have replotted the data in Figure 8a in terms of Γ scaled with respect to Γ_0; see Figure 8b. Such a comparison, in fact, reveals discrepancies not evident in Figure 8a. For example, we observe from our simulations that (for $N = 200$) a crossover from attraction to steric repulsion occurs at $\Gamma/\Gamma_0 \approx 0.85$. According to the numerical mean-field calculations, this crossover occurs at a value of Γ/Γ_0 slightly larger than 1.0. In general, one would expect a better agreement between the simulations and the mean-field theories for larger coverages (i.e., oversaturated surfaces), where spatial fluctuations in segment density are expected to be less pervasive. We plan to examine this in a future communication.

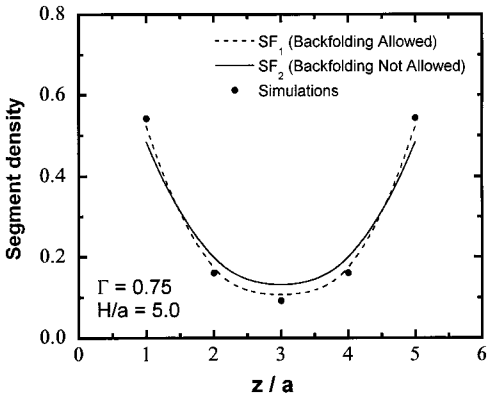

Figure 9. Segment density profile between two adsorptive walls. The coverage in each surface is $\Gamma = 0.75$, and the separation between walls is $H/a = 5$.

An observation concerning for what values of Γ/Γ_0 the crossover from attraction to repulsion occurs is in order. As $N \rightarrow \infty$, the mean-field calculations (based on both the two-order-parameter theory of Semenov and Joanny[7] and the SF theory) predict steric repulsion for $\Gamma/\Gamma_0 = 1.0$ for all values of H. However, this steric repulsion turns into attraction even for very low undersaturations (i.e., even for small deviations below 1.0). For instance, the two-order-parameter theory predicts attraction for any $\Gamma/\Gamma_0 \lesssim 0.98$. It is interesting to contrast the above mean-field prediction with that of the scaling/free energy functional theory, which shows a sharp crossover from steric repulsion to attraction at a rather low value of Γ/Γ_0 (0.4). As we pointed out earlier, in our simulations we observe the crossover at $\Gamma/\Gamma_0 \approx 0.85$ for $N = 200$. It would, therefore, be interesting to extend the simulations to longer chain lengths to examine whether the asymptotic prediction of the scaling/free energy functional theory is reached.[45]

It is also important to mention that the discrepancies between the simulations and the mean-field predictions are not surprising because of the large density fluctuations that exist in undersaturated polymer layers in good solvents. Nevertheless, an analysis of the differences between the SF theory and the simulations (for both undersaturated and saturated surfaces), and efforts to improve the numerical mean-field predictions, are important since, as mentioned earlier, the numerical mean-field theory provides the only *easily accessible* guidelines for the structure and forces induced by "short" physisorbed polymers. In this context, it is interesting to make a final comparison between SF_1 and SF_2. In Figure 9 we show the overall density profile obtained for $\Gamma = 0.75$ and $H/a = 5$. The agreement observed here between SF_1 and simulations is fortuitous. Although the two density profiles (those obtained from SF_1 and simulations) are almost identical, the corresponding forces are drastically different from each other (see Figure 7). This illustrates the fact that agreements in segment density profiles or surface coverage alone are not sufficient as a measure of the acceptability of the theoretical approximations. Finally, SF_2 predicts a larger concentration at the midpoint between the surfaces (partly due to the prediction of a larger number of bridges). However, it underestimates the segment concentration at the surface. It would therefore be interesting to extend the numerical mean-field calculations to also incorporate bond correlations. This correction, which leads to the so-called self-consistent anisotropic theory, attempts to improve over the random mixing approximation in each layer, and hence, improve the numerical predictions.

4. Concluding Remarks

We have presented, to the best of our knowledge, the first computer simulations that directly link the structure of a physisorbed layer to the induced forces. The structure (number and size) of the bridges in undersaturated layers is qualitatively described by the scaling analysis of Ji et al.,[38] but their predictions for the bridging force are strictly valid only for very low coverages, where the polymer layer consists of isolated polymer chains. In this regime each bridge behaves as a strongly stretched chain, which can be described by the Pincus law of elasticity. As the coverage increases, steric repulsion sets in, and the net force is given by a balance between bridging attraction and steric repulsion. Close to the saturation coverage, the steric repulsion overcomes the bridging attraction completely and the forces become repulsive at all separations. For chain length $N = 200$, the value of Γ/Γ_0 at which this crossover from attraction to repulsion occurs is, approximately, 0.85. Additional simulations with longer polymer chains are required to examine whether the results approach the asymptotic predictions (for long chain lengths) given by the scaling/free energy functional theory. We have also initiated a systematic comparison of the structure and forces obtained from computer simulations and those predicted from lattice numerical mean-field theories. The use of a second-order Markov chain improves the predictions substantially as compared to the standard first-order Markov formulation (in particular, the predictions on the structure of the layer). This comparison should be extended for different chain lengths for both undersaturated and oversaturated surfaces.

Acknowledgment. The authors thank Professor Andrey Milchev of the Bulgarian Academy of Sciences for discussions and suggestions on the manuscript. The authors acknowledge partial financial support from the National Science Foundation through the Engineering Research Center for Particle Science and Technology at the University of Florida (Grant NSF EEC-9402989).

References and Notes

(1) de Gennes, P.-G. *Macromolecules* **1981**, *14*, 1637.
(2) de Gennes, P.-G. *Macromolecules* **1982**, *15*, 492.
(3) Ingersent, K.; Klein, J.; Pincus, P. A. *Macromolecules* **1990**, *23*, 548.
(4) Klein, J.; Pincus, P. A. *Macromolecules* **1982**, *15*, 1129.
(5) Ingersent, K.; Klein, J.; Pincus, P. A. *Macromolecules* **1986**, *19*, 1374.
(6) Semenov, A. N.; Bonet-Avalos, J.; Johner, A.; Joanny, J.-F. *Macromolecules* **1996**, *29*, 2179.
(7) Semenov, A. N.; Joanny, J.-F.; Johner, A.; Bonet-Avalos, J. *Macromolecules* **1997**, *30*, 1479.
(8) Semenov and Joanny[6,7] write the interaction energy between the segments solely in terms of the second virial coefficient. This assumption is valid under the so-called marginal conditions, which lie somewhere between the semidilute and the concentrated regimes.[17]
(9) de Gennes, P.-G. *Scaling Concepts in Polymer Physics*; Cornell University Press: Ithaca, NY, 1979.
(10) de Gennes, P.-G. In *Physical Basis of Cell−Cell Adhesion*; Bongard, P., Ed.; CRC Press Inc.: Boca Raton, FL, 1988.
(11) Rossi, G.; Pincus, P. A. *Europhys. Lett.* **1988**, *5*, 641.
(12) Rossi, G.; Pincus, P. A. *Macromolecules* **1989**, *22*, 276.
(13) Klein, J.; Rossi, G. *Macromolecules* **1998**, *31*, 1979.
(14) Scheutjens, J. M. H. M.; Fleer, G. J. *J. Phys. Chem.* **1979**, *83*, 1619; *Macromolecules* **1985**, *18*, 1882.
(15) Johner, A.; Bonet-Avalos, J.; van der Linden, C. C.; Semenov, A. N.; Joanny, J. F. *Macromolecules* **1996**, *29*, 3629.

(16) Fleer, G. J.; van Male, J.; Johner, A. *Macromolecules* **1999**, *32*, 825.
(17) Fleer, G.; Cohen Stuart, M.; Scheutjens, J.; Cosgrove, T.; Vincent, B. *Polymers at Interfaces*; Chapman and Hall: London, 1993.
(18) Leermakers, F. A. M.; Scheutjens, J. M. H. M.; Gaylord, R. J. *Polymer* **1984**, *25*, 1577.
(19) van der Linden, C. C.; Leermakers, F. A. M.; Fleer, G. J. *Macromolecules* **1996**, *29*, 1172.
(20) Leermakers, F. A. M.; Scheutjens, J. M. H. M. *J. Chem. Phys.* **1988**, *89*, 6912.
(21) Leermakers, F. A. M.; Lyklema, J. *Colloids Surf.* **1992**, *67*, 239.
(22) de Joannis, J.; Bitsanis, I. *Langmuir*, in press.
(23) Siepmann, J. I.; Frenkel, D. *Mol. Phys.* **1992**, *75*, 59.
(24) Jimenez, J.; Rajagopalan, R. *Eur. Phys. J. B* **1998**, *5*, 237.
(25) Jimenez, J. Ph.D. Thesis, University of Florida, Gainesville, FL, 2000.
(26) de Joannis, J.; Jimenez, J.; Rajagopalan, R.; Bitsanis, I. *Europhys. Lett.* **2000**, *51*, 41.
(27) Jimenez, J.; de Joannis, J.; Bitsanis, I.; Rajagopalan, R. *Macromolecules* **2000**, *33*, 7157.
(28) de Joannis, J.; Jimenez, J.; Rajagopalan, R.; Bitsanis, I. *Macromolecules*, submitted.
(29) This value of N is not sufficient to test the scaling limit,[22] and hence, we will not be able to make definite comparisons with the "scaling" free energy functional used by Rossi and Pincus.[11,12]
(30) Binder, K. In *Monte Carlo and Molecular Dynamics Simulations in Polymer Science*; Binder, K., Ed.; Oxford University Press: New York, 1995.
(31) Rosenbluth, M. N.; Rosenbluth, A. W. *J. Chem. Phys.* **1955**, *23*, 356.
(32) Allen, M. P.; Tildesley, D. J. *Computer Simulations of Liquids*; Clarendon Press: Oxford, 1987.
(33) The force calculated from eq 2 corresponds to the so-called restricted equilibrium case,[9,17] i.e., the case where the number of polymer chains within the gap remains constant during the compression.
(34) Jimenez, J.; Rajagopalan, R. *Langmuir* **1998**, *14*, 2598.
(35) We actually proceed in the reverse order from step iii to step i since in that case one can use the final configuration from step iii as the initial configuration for step i, thus reducing the time required to generate a new system.
(36) In most of the cases one additional simulation with a repulsive potential $U_{ext}(H) = 0.20\ k_BT$ is enough to get a good estimate of $P(0)$. However, when the chains are strongly confined, additional simulations with stronger repulsive potentials may be required. For example, for the data shown in Figure 1, four simulations with $U_{ext}(H) = 0.20$, 0.40, 0.60, and 0.80 k_BT were required to obtain the force when moving the wall from $H = 5$ to $H = 4$.
(37) We have performed simulations for the same surface coverage but with a larger simulation box ($L = 80$ and $n = 32$), and we obtained essentially the same results.[28]
(38) Ji, H.; Hone, D.; Pincus, P.; Rossi, G. *Macromolecules* **1990**, *23*, 698.
(39) Pincus, P. *Macromolecules* **1976**, *9*, 386.
(40) We use $C \approx 3.2$, as has been found from simulations on chains with hard-core excluded volume.[41,42]
(41) Pierleoni, C.; Arialdi, G.; Ryckaert, J. P. *Phys. Rev. Lett.* **1997**, *79*, 2990.
(42) Titantah, J. T.; Pierleoni, C.; Ryckaert, J. P. *Phys. Rev. E* **1999**, *60*, 7010.
(43) Calculations based on the *average* number and *average* size of the bridges are roughly 10% lower than the ones shown in Figure 4, which are calculated using the entire number and size distribution of bridges.
(44) Wang, Y.; Mattice, W. L. *Langmuir* **1994**, *10*, 2281.
(45) It is not clear what the limitations of the "scaling-based" free energy functional proposed by de Gennes[1] are. Examination of the extensions of this theory for the case of undersaturated layers is, therefore, highly relevant.

MA0011237